Egypt. J. Chem. Vol. 68, SI: Z. M. Nofal, pp. 289 - 306 (2025)

Egyptian Journal of Chemistry

http://ejchem.journals.ekb.eg/

Synthesis, Antimicrobial Activity and Molecular Docking of Novel Series of Phthalazine Derivatives

Marwa M. Rezk [*a], A. A. F. Wasfy[a], Mohamed S. Behalo[a], Samar El-Kalyoubi[b], Aly A. Aly[a]

[a] *Chemistry Department, Faculty of Science, Benha University, Benha. P.O. Box 13518, Egypt*

[b] *Pharmaceutical Organic Chemistry, Faculty of Pharmacy, Port Said University, Port Said, P.O. Box 42511, Egypt*

Abstract

A straightforward and effective method for synthesizing phthalazine derivatives was developed through the reaction of 1-(4-(4-chlorophthalazin-1-yl) phenyl]-pyrrolidine-2,5-dione **(3),** a key precursor, with various nucleophiles containing carbon, nitrogen, oxygen, and sulfur. The structures of all synthesized compounds were verified through elemental analysis and spectral data. Furthermore, certain derivatives were assessed for their antibacterial and antifungal activities and compared with standard drugs. Among them, compounds **4, 14a, 15,** and **18** demonstrated antimicrobial activity, positioning them as promising candidates for therapeutic use. In vitro testing demonstrated their potent efficacy against bacterial strains (*Escherichia Coli*, *Staphylococcus Aureus*) and fungal pathogens (*Aspergillus Niger*), indicating broad-spectrum antimicrobial potential. Molecular docking analyses supported these findings, revealing strong binding interactions with key microbial enzymes, which align with their observed inhibitory effects.

Keywords; Phthalazin-1-(*2H*)-one, Chlorophthalazine, Pyrrolidine-2,5-dione, A ntimicrobial activity, Molecular docking

Introduction

Biologically essential molecules, such as DNA, RNA, and vitamins, frequently contain heterocyclic core rings. These structural motifs play a fundamental role in numerous biochemical and physiological processes, making them indispensable to life. Their unique electronic and steric properties contribute to crucial biological functions, including enzymatic regulation, signal transduction, and genetic information storage. The significance of heterocyclic systems has driven advancements in medicinal chemistry, particularly in the synthesis of novel therapeutic agents [1-5]. Among these, Phthalazines, a class of nitrogen-containing heterocycles, have attracted significant attention for their wide-ranging pharmacological activities, particularly in cancer drug development [6]. Among them, 4-substituted phthalazine derivatives have shown diverse therapeutic potential, such as anti-inflammatory [7-8], antimicrobial [9-14], antitumor agents [15-18], anticonvulsant, and vasorelaxant effects [19-20]. Moreover, phthalazine-based scaffolds, including aminophthalazine and hydrazinylphthalazine derivatives, are found in some drugs, as shown in Figure 1[2], such as hydralazine [21] and carbazeran [22- 23]. Azelastine also functions as an antihistamine for treating allergic rhinitis [24]. Vatalanib and ZD 6474 [25-26], which have shown promise in inhibiting tumour progression.

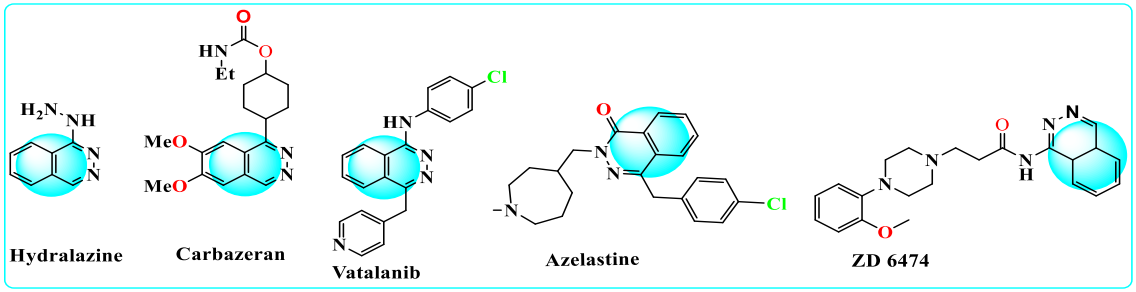

***Figure 1*: Some drugs based on the phthalazine moiety**

Additionally, the phthalazine ring has demonstrated efficacy as a robust scaffold in designing melatonin MT1 and MT2 ligands, acting as bio isosteric analogs of agomelatine, a compound known for its role in regulating circadian rhythms and antidepressant

*Corresponding author e-mail: Marwa_3336@yahoo.com.; (Marwa Mohamed Rezk).
Received date 13 March 2025; Revised date 10 April 2025; Accepted date 13 May 2025

DOI: 10.21608/EJCHEM.2025.361774.11447

activity [27]. Despite significant progress in antimicrobial drug development, the continuous emergence of resistant microorganisms remains a critical challenge, highlighting the need for novel and more potent therapeutic agents [28-35]. In response, medicinal chemists have focused on designing small molecules capable of overcoming resistance mechanisms. Phthalazine derivatives, with their diverse structural modifications, have shown promise in this regard, displaying activity against Gram-positive and Gram-negative bacteria, fungi, and even mycobacterial infections. In this context, molecular docking has become an essential computational tool for predicting the interactions between small molecules and protein targets, offering valuable visions into binding affinity and biological activity, which are crucial for rational drug design. Advances in docking algorithms have further refined the accuracy of interaction predictions, facilitating the identification and optimization of promising drug candidates [36]. These studies help assess binding interactions and potential biological effects, thereby establishing a foundation for evaluating the therapeutic relevance of newly synthesized compounds [37-39]. Building upon these insights, our study focuses on the synthesis of novel phthalazine derivatives incorporating a pyrrolidine-2,5-dione moiety, a pharmacophore known for its significant bioactivity in antimicrobial and anticancer agents. By integrating this moiety into the phthalazine core, we aim to enhance the biological profile of these derivatives. Furthermore, we conducted molecular docking studies to investigate their potential interactions with key microbial and enzymatic targets, thereby evaluating their pharmaceutical potential

2. Materials and Methods

2.1 Materials

All chemical reagents utilized in this study were sourced from Sigma-Aldrich, while analytical-grade solvents were procured from El-Nasr Chemicals Company. The melting points of the synthesized compounds were determined using a Gallen-Kamp melting point apparatus, with all reported values remaining uncorrected. For spectroscopic characterization, infrared (IR) spectra were recorded using potassium bromide (KBr) pellets on a ThermoFisher Nicolet iS10 FT-IR spectrometer. Nuclear Magnetic Resonance (NMR) spectroscopy was performed in dimethyl sulfoxide (DMSO-d_6) as the solvent. ^{1}H NMR spectra were recorded at 400 MHz and ^{13}C NMR spectra at 100 MHz using a Bruker NMR spectrometer. Additionally, high-resolution ^{1}H and ^{13}C NMR spectra were acquired at 500 MHz and 125 MHz on a Jeol Resonance spectrometer, with tetramethylsilane (TMS) serving as the internal reference. All chemical shifts were reported in delta (δ) values, expressed in parts per million (ppm). For mass spectrometric analysis, data were obtained via direct inlet injection, interfaced with a Thermo Scientific GC/MS model ISQ. The antimicrobial activity of the synthesized compounds was evaluated at the Micro Analytical Center, Cairo University.

2.2 Synthesis

4-(4-Aminophenyl) phthalazin-1-(2*H*)-one (1)

A solution of 2-(4-aminobenzoyl)-benzoic acid (10 mmol) in 15 ml of absolute ethanol was added (240 mmol) hydrazine hydrate. The reaction mixture was heated under reflux for 6 hours [15-16]. After cooling, the reaction mixture was filtered off and crystallized from DMF/H_2O mixture to give **1** as pale brown crystalline. Yield 50%. M p 250 – 252°C. IR [KBr, cm^{-1}]: 3400, 3254, 3156, 3100 (NH~OH, NH_2), 1666 (C=O). ^{1}H-NMR [DMSO-d_6, 500 *MHz*, δ, ppm]: 7.24 – 7.57 (m, 8H, aromatic protons), 9.96 (s, 2H, NH_2, exch..), 13.15 (s, 1H, NH~OH, exch..). ^{13}C NMR [DMSO-d_6, 125 *MHz*, δ, ppm]: 159.15, 137.14, 134.74, 134.58, 133.09, 131.92, 131.56, 128.90, 128.36, 128.12, 127.47, 126.55, 125.56, 123.46(aromatic carbons). Ms, m/z = 237 ($M^{\bullet+}$, 21.44%). *Anal*. Calcd. for $C_{14}H_{11}N_3O$ (237.26): C, 70.87 %; H, 4.67%; N,17.71%; O, 6.74 %. Found, 70.85%.; H, 4.69%.; N, 17.70; %. O, 6.79 %.

1-(4-(4-Oxo-3,4-Dihydrophthalazin-1-yl) phenyl)-pyrrolidine-2,5-dione (2)

An equimolar amount of compound 1 (10 mmol) was fused with succinic anhydride (10 mmol) at 250°C for 2 hours. After cooling, the precipitate was triturated with H_2O, the resultant mixture was filtered off and recrystallized from ethanol to give **2** as pale yellow crystals. Yield 90%. M p 203 - 205°C. IR [KBr, cm^{-1}]: 3467, 3158 (OH, NH), 1780, 1668 (C=O), 1595 (C=N). ^{1}H NMR [DMSO-d_6, 500 *MHz*, δ, ppm]: 2.02 (m, 4H, $2CH_2$), 6.98 –7.56 (m, 8H, aromatic protons), 9.92 (s, 1H, NH, exch.), 12.88 (s, 1H, OH, exch..). ^{13}C NMR [DMSO-d_6, 100 *MHz*, δ, ppm]: 167.48, 159.58, 137.57, 135.18, 135.02, 133.52, 132.38, 132.01, 129.32, 128.82, 128.54, 127.88, 126.99, 125.99, 123.89 (CO and aromatic carbons), 29.26 ($2CH_2$). Ms, m/z = 319 ($M^{\bullet+}$, 36.26%). *Anal*. Calcd. for $C_{18}H_{13}N_3O_3$ (319.32):C, 67.71%.; H, 4.10%.; N, 13.16%.O, 15.03%. Found C, 67.65%.; H, 4.20%.; N, 13.20%.; O, 15.115%.

1-(4-(4-Chlorophthalazin-1-yl) phenyl)pyrrolidine-2,5-dione (3)

A mixture of phosphorus pentachloride (10 mmol), phosphorus oxychloride (20 mmol), and phthalazinone **2** (10 mmol) was heated under reflux in a water bath for 4 hours. then reaction mixture was cooled and poured onto crushed ice. The resulting solid was filtered off, washed several times with water, dried, and crystallized from

ethanol to give **3** as off-white crystals. Yield 80%. M p 233 – 235°C. IR (KBr, cm^{-1}) : 3020 (CH- aromatic), 2890 (CH-aliphatic), 1765 - 1662 (C=O), 1601 (C=N), 709 (C-Cl). ^{1}H NMR (DMSO-d_6, 500 MHz, δ, ppm): 2.03 (m, 4H, $2CH_2$), 7.28 – 7.94 (m, 8H, aromatic protons). ^{13}C NMR (DMSO-d_6, 125 MHz, δ, ppm): 167.07, 159.15, 137.14, 134.75, 134.60, 133.10, 131.58, 128.90, 128.37, 128.82, 128.12, 127.48, 126.55, 125.57, 123.46 (CO and aromatic carbons), 28.82 (CH_2). Ms, m/z = 337 ($M^{\bullet+}$, 14.66%), 338 (M^{+1}, 17.64%). *Anal*. Calcd. for $C_{18}H_{12}ClN_3O_2$ (337.76): C, 64.01%; H, 3.58%; Cl, 10.50%; N, 12.44%; O, 9.47%. Found: C, 63.98%; H, 3.50%; Cl, 10.55%; N, 12.49%; O, 9.40%.

1-(4-(4-Methoxyphthalazin-1- yl)phenyl)pyrrolidine-2,5-dione (4)

A solution of compound **3** (10 mmol) in methanol (30 ml) containing sodium methoxide (0.54 g, 10 mmol) was refluxed for 6 hours. After cooling, the reaction mixture was poured into an ice/HCl solution. The resulting solid was filtered off and crystallized from ethanol to furnish **4** as pale brown crystals. Yield 60%. M p 170 – 172°C. IR (KBr, cm^{-1}): 2920, 2868 (CH- aliphatic), 1706 - 1660 (C=O), 1383 (C-O-C), 1591 (C=N).^{1}H NMR (DMSO-d_6, 500 MHz, δ, ppm): 2.09 (m, 4H, $2CH_2$), 4.45 (s, 3H, CH_3), 7.90 – 8.04 (m, 8H, aromatic protons). ^{13}C NMR (DMSO-d_6, 125 MHz, δ, ppm): 170.08, 167.07, 159.15, 137.14, 134.75, 134.61, 133.11, 131.92, 131.58, 128.89, 128.37, 128.11, 127.48, 126.55, 125.58, 123.46 (CO and aromatic carbons), 54.50(CH_3), 28.72 ($2CH_2$). Ms, m/z = 333 ($M^{\bullet+}$, 29.98%). *Anal*. Calcd. for $C_{19}H_{15}N_3O_3$ (333.35): C, 68.46%; H, 4.54%; N, 12.61%; O, 14.40%. Found: C, 68.40%; H, 4.50%; N, 12.68%; O, 14.45%.

1-(4-(Tetrazolo[5,1-a]phthalazin-6-yl)phenyl)pyrrolidine-2,5-dione (5)

Sodium azide (10 mmol) was added to a solution of chlorophthalazine **3** (10 mmol) in DMSO (20 mL) and heated under reflux for 2 hours. After cooling, the reaction mixture was poured onto ice. The resulting precipitate was filtered off and crystallized from ethanol to afford **5** as pale brown crystals. Yield 65%. M p 216 – 218°C. IR (KBr, cm^{-1}) : 3052 (CH- aromatic), 2955, 2890 (CH-aliphatic), 1779 - 1668 (C=O), 1591 (C=N). ^{1}H NMR (DMSO-d_6, 400 MHz, δ, ppm): 2.05 (m, 4H, $2CH_2$) 7.43 – 8.30 (m, 8H, aromatic protons). ^{13}C NMR (DMSO-d_6, 125 MHz, δ, ppm): 167.04, 159.13, 137.12, 134.73, 134.57, 133.08, 131.91, 131.56, 128.87, 128.35, 128.09, 127.46, 126.53, 125.55, 123.44(CO and aromatic carbons), 28.80($2CH_2$). Ms, m/z = 344 ($M^{\bullet+}$, 13.95%) *Anal*. Calcd. for $C_{18}H_{12}N_6O_2$ (344.33): C, 62.79%; H, 3.51%; N, 24.41%; O, 9.29%. Found: C, 62.85%; H, 3.40%; N, 24.50%; O, 9.15%.

1-(4-(4-((2-Hydroxyethyl) amino)phthalazin-1-yl)phenyl)pyrrolidine-2,5-dione (6)

A solution of chlorophthalazine **3** (10 mmol) in dioxane (40 mL) containing ethanolamine (10 mmol) was heated under reflux for 12 hours. The reaction mixture was concentrated, and the resulting solid was triturated with water, filtered off, and crystallized from ethanol to give **6** as pale brown crystals. Yield 70%. M p 282 – 284°C. IR (KBr, cm^{-1}): 3445 (OH), 3332 (NH), 2926, 2852 (CH -aliphatic), 1780 - 1626 (C=O), 1588 (C=N). ^{1}H NMR (DMSO-d_6, 500 MHz, δ, ppm): 2.07 (m, 4H, $2CH_2$), 3.66 – 4.40 (m, 4H, $2CH_2$), 7.19 – 8.64 (m, 8H, aromatic protons), 10.89 (s, 1H, NH, exch.), 12.90 (s, 1H, OH, exch.).^{13}C NMR (DMSO-d_6, 125 MHz, δ, ppm) 167.08, 163.40, 162.95, 154.76, 136.30, 136.19, 134.73, 132.65, 131.96, 131.56, 130.74, 128.93, 128.14, 127.49, 127.19, 125.20, 124.84, 124.76, 123.46 (CO and aromatic carbons), 28.53, 26.68, 26.60 (aliphatic carbons). Ms, m/z = 362 ($M^{\bullet+}$, 27.16%). *Anal*. Calcd. for $C_{20}H_{18}N_4O_3$ (362.39): C, 66.29%; H, 5.01%; N, 15.46%; O, 13.25%. Found: C, 66.20%; H, 4.98%; N, 15.40%; O, 13.20%.

1-(4-(2,3-Dihydroimidazo[2,1-a]phthalazin-6-yl)phenyl)pyrrolidine-2,5-dione (8)

A mixture of compound **6** (10 mmol) and thionyl chloride (2 mL) in anhydrous benzene (30 mL) was heated under reflux for 2 hours, after which the solvent was evaporated under reduced pressure. The resulting solid residue was dissolved in 10% potassium carbonate (20 cm^3) and then extracted with chloroform. After evaporating the chloroform, free base **8** was obtained and crystallized from ethanol. Yield 60%. M p 318 - 320°C. IR (KBr, cm^{-1}): 3073 (CH - aromatic), 2961, 2898 (CH-aliphatic), 1778 - 1682 (C=O), 1592 (C=N). ^{1}H NMR (DMSO-d_6, 500 MHz, δ, ppm): 2.05 (m, 4H, $2CH_2$), 3.72 – 5.52 (m, 4H, $2CH_2$), 7.41 – 8.12 (m, 8H, aromatic protons) Ms, m/z = 345 (M^{+1}, 12.23 %). *Anal*. Calcd. for $C_{20}H_{16}N_4O_2$ (344.37): C, 69.76%; H, 4.68%; N, 16.27%; O, 9.29%, Found: C, 69.70%; H, 4.80%; N, 16.27%; O, 9.35%.

1-(4-(4-Mercaptophthalazin-yl) phenyl) pyrrolidine-2,5-dione (9)

A solution of compound **3** (10 mmol), thiourea (0.76 g, 10 mmol) in ethanol (20 mL) containing sodium ethoxide (10 mmol) was heated under reflux for 6 hours. The mixture was poured onto ice-water and acidified with acetic acid. The resulting solid was filtered off, dried, and crystallized from ethanol to give **9** as pale brown crystals. Yield 60%. M p 212-214°C. IR (KBr, cm^{-1}): 2553 (SH), 1775 - 1661 (C=O), 1592 (C=N), 1349 (C=S). ^{1}H NMR (DMSO-d_6, 400 MHz, δ, ppm): 2.04 (m, 4H, $2CH_2$), 7.44 - 8.29 (m, 8H, aromatic protons), 12.88 (s, 1H, SH exch..). ^{13}C NMR (DMSO-d_6, 125 MHz, δ, ppm): 167.08, 159.15, 137.15, 134.75, 134.62, 133.11, 131.59, 128.89, 128.38, 128.12, 127.49, 126.56, 125.59, 123.47 (CO and aromatic carbons), 28.51($2CH_2$). Ms, m/z = 335 ($M^{\bullet+}$, 64.96%). *Anal*. Calcd. for $C_{18}H_{13}N_3O_2S$ (335.38): C, 64.46%; H, 3.91%; N, 12.53%; O, 9.54%; S, 9.56%. Found: C, 64.40%; H, 4.01%; N, 12.50%; O, 9.49%; S, 9.50%.

(4-(4-(2,5-Dioxopyrrolidin-1-yl) phenyl)phthalazin-1-yl)glycine (10)

A mixture of compound **3** (10 mmol) and glycine (10 mmol), in pyridine (4 mL) containing a few drops of water, was heated under reflux for 3 hours. The mixture was poured onto an ice-HCl solution. The resulting solid was filtered off, washed with water, and crystallized from acetic acid to give **10** as pale brown crystals. Yield 75%. M p 211– 213°C. IR (KBr, cm^{-1}): 3449 (OH), 3166 (NH), 3004 (CH- aromatic), 2924, 2854 (CH- aliphatic), 1775 - 1665 (C=O), 1594 (C=N). ^{1}H NMR (DMSO-d_6, 400 MHz, δ, ppm): 2.04 (m, 4H, $2CH_2$), 3.80 (s, 2H, CH_2), 4.43 (s, 1H, NH exch..), 6.83 – 7.93 (m, 8H, aromatic protons), 10.88 (s, 1H, OH exch..). ^{13}C NMR (DMSO-d_6, 125 MHz, δ, ppm): 167.07, 163.45, 159.76, 137.30, 134.75, 132.62, 131.90, 131.52, 130.71, 128.91, 128.11, 127.50, 127.20, 125.22, 124.86, 124.77, 123.44 (CO and aromatic carbons), 28.53, 26.70 (aliphatic carbons). Ms, m/z = 376 ($M^{\bullet+}$, 40.72%). *Anal*. Calcd. for $C_{20}H_{16}N_4O_4$ (376.37): C, 63.83%; H, 4.29%; N, 14.89%; O, 17.00%; Found: C, 63.77%; H,4.40%; N, 14.50%; O, 16.95%.

1-(4-(3-Oxo-2,3-dihydroimidazo[2,1-a]phthalazin-6-yl)phenyl)pyrrolidine-2,5-dione (11)

Acid 8 (10 mmol) was refluxed in acetic anhydride (15 mL) for 3 hours. The reaction mixture was cooled and poured onto ice. The resulting solid was filtered off, washed with water, and crystallized from ethanol to furnish 11 as pale brown crystals. Yield 80%. M p 180 –182°C. IR (KBr, cm^{-1}): 3052 (CH - aromatic), 2945, 2859 (CH-aliphatic), 1777 - 1655 (C=O), 1592 (C=N). ¹). ¹H NMR (DMSO-d_6, 500 MHz, δ, ppm): 2.01 (m,4H, 2CH2), 4.45 (s, 2H, CH_2), 7.43 – 7.97 (m, 8H, aromatic protons). Ms, m/z = 358 ($M^{\bullet+}$, 32.20%), 359 (M^{+1}, 55.21%). *Anal*. Calcd. for $C_{20}H_{14}N_4O_3$ (358.36): C, 67.03%; H, 3.94%; N, 15.63%; O, 13.39%; Found: C, 67.10%; H, 3.86%; N, 15.50%; O, 13.5%.

1-(4-(8-Oxo-8H-phthalazino[1,2-b]quinazolin-5-yl) phenyl)pyrrolidine-2,5-dione (12)

A mixture of compound 3 (10 mmol) and anthranilic acid (10 mmol) was subjected to fusion in an oil bath at 190 – 191°C for 2 hours. Then the reaction mixture was cooled and poured into 40 mL of cold water. The resulting solid was filtered off and crystallized from ethanol to give 12 as pale brown crystals. Yield 80%. M p 258 - 260°C. IR (KBr, cm-1): 3071 (CH-aromatic), 2945 (CH-aliphatic), 1779 - 1699 (C=O), 1576 (C=N).¹H NMR (DMSO-d_6, 400 MHz, δ, ppm): 2.03 (m, 4H, $2CH_2$), 7.52 – 8.93 (m, 12H, aromatic protons). Ms, m/z = 421 ($M^{\bullet+}$, 26.84%). *Anal*. Calcd. for $C_{25}H_{16}N_4O_3$ (421.43): C, 71.42%; H, 3.84%; N, 13.33%; O, 11.42%; Found: C, 71.46%; H, 3.89%; N, 13.35%; O, 11.44%.

1-(4-(4-Aminophthalazin-1-yl)phenyl)pyrrolidine-2,5-dione (13)

A mixture of chlorophthalazine **3** (10 mmol) and ammonium acetate (10 mmol) was heated for 2 hours. After cooling, the reaction mixture was triturated with distilled water, then the resultant solid was filtered off, dried, and crystallized from ethanol to give **13** with a yield of 82%. M p 221–223°C. IR (KBr, cm^{-1}): 3373, 3220 (NH_2), 3046 (CH - aromatic), 2919, 2850 (CH- aliphatic), 1774 – 1656 (C=O), 1586 (C=N). ¹H NMR (DMSO-d_6, 400 MHz, δ, ppm): 2.04 (m, 4H, $2CH_2$), 7.44 – 8.29 (m, 8H, aromatic protos), 12.88 (s, 2H, NH_2, exch..). ^{13}C NMR spectrum (DMSO-d_6, 100 MHz, δ, ppm): 167.49, 159.58, 137.57, 135.18, 135.02, 133.52, 132.38, 132.01, 129.32, 128.82, 128.54, 127.88, 126.99, 125.99, 123.89 (CO and aromatic carbons) 31.16 ($2CH_2$). Ms, m/z =318 ($M^{\bullet+}$, 18.84%). *Anal*. Calcd. for $C_{18}H_{14}N_4O_2$ (318.31): C, 67.91%; H, 4.43%; N, 17.60%; O, 10.05%; Found: C, 67.88%; H, 4.46%; N, 17.59%; O, 10.10%.

General procedures for synthesis of compounds 14a-b

A solution of chlorophthalazine **3** (10 mmol), *p*-phenylenediamine, and *p*-aminophenol (each 10 mmol) in benzene (40 mL) was heated under reflux for 5 hours. The reaction mixture was then concentrated by evaporation. The obtained solid product was then crystallized from ethanol to furnish 14a and **14b**, respectively.

1-(4-(4-((4-Aminophenyl)amino)phthalazin-1-yl)phenyl)pyrrolidine-2,5-dione (14a)

Yield 70%. M p 209 - 211°C. The IR (KBr, cm^{-1}): 3449, 3335, 3161 (NH_2, NH), 3007 (CH- aromatic), 2950, 2897 (CH -aliphatic), 1780 - 1668 (C=O), 1595 (C=N). ^{1}H NMR spectrum (DMSO-d_6 ,400 MHz, δ, ppm): 2.03(m, 4H, $2CH_2$), 6.90 - 8.30 (m, 12H, aromatic protons), 9.91 (s, 2H, NH_2, exch.), 12.88 (s, 1H, NH exch.). ^{13}C NMR (DMSO-d_6, 125 MHz, δ, ppm): 167.05, 159.75, 137.61, 136.77, 134.18, 134.05, 133.53, 132.36, 131.98, 128.33, 128.29, 127.55, 127.93, 127.87, 125.99, 124.99, 123.42 (CO and aromatic protons), 29.03 ($2CH_2$). Ms, m/z = 409 ($M^{\bullet+}$, 38.62%). *Anal*. Calcd. for $C_{24}H_{19}N_5O_2$ (409.45): C, 70.40%; H, 4.68%; N, 17.10%; O, 7.82%; Found: C, 70.50%; H, 4.25%; N, 17.10%; O, 17.75 %.

1-(4-(4-((4-Hydroxyphenyl)amino)phthalazin-1-yl)phenyl)pyrrolidine-2,5-dione (14b)

Yield 68%. M p 219 - 221°C. IR (KBr, cm^{-1}): 3446 (OH), 3102 (NH), 3051 (CH-aromatic), 2924, 2854 (CH-aliphatic), 1778 - 1701 (C=O), 1592 (C=N). ^{1}H NMR spectrum (DMSO-d_6, 500 MHz, δ, ppm): 2.02 (m. 4H, $2CH_2$), 7.42 –8.26 (m, 12H, aromatic protons), 9.80 (s,1H, NH exch.), 12.84 (s, 1H, OH exch..). Ms, m/z = 410 ($M^{\bullet+}$, 25.36%). *Anal*. Calcd. for $C_{24}H_{18}N_4O_3$ (410.43): C, 70.23%; H, 4.42%; N, 13.65%; O, 11.69%; Found: C, 70.15%; H, 4.49%; N, 13.60%; O,11.60%.

1-(4-(3-Amino-[1,2,4]triazolo[3,4-a]phthalazin-6-yl)phenyl)-pyrrolidine-2,5-dione (15)

Thiosemicarbazide (10 mmol) in absolute ethanol and compound **3** (10 mmol) were heated under reflux for 6 hours. After cooling, the obtained solid was filtered, dried, and crystallized from ethanol to afford compound **15**. Yield 83%. M p 354 – 356°C. IR (KBr, cm^{-1}): 3465, 3163 (NH_2), 3053 (CH- aromatic), 2925, 2896 (CH- aliphatic), 1775 - 1665 (C=O), 1598 (C=N). ^{1}H NMR (DMSO-d_6, 500 MHz, δ, ppm): 2.07 (m, 4H, $2CH_2$), 7.44 – 8.12 (m, 8H, aromatic protons). 11.56 (s, 2H, NH_2, exch..), ^{13}C NMR (DMSO-d_6, 125 MHz, δ, ppm) 167.08, 159.16, 137.18, 134.77, 134.64, 133.14, 131.59, 128.92, 128.39, 128.14, 127.50, 126.58, 125.61, 123.49, 30.01($2CH_2$). Ms, m/z = 358 ($M^{\bullet+}$, 60.61%), *Anal*. Calcd. for $C_{19}H_{14}N_6O_2$ (358.35): C, 63.68%; H, 3.94%; N, 23.45%; O, 8.93%. Found: C, 63.70%; H, 3.90%; N, 23.50%

Ethyl2-cyano-2-(4-(4-(2,5-dioxopyrrolidin-1-yl)phenyl)phthalazin-1-yl)acetate (16)

A mixture of compound **3** (10 mmol) and ethylcyanoacetate (10 mmol) in ethanol containing sodium ethoxide was heated under reflux for 6 hours. The reaction mixture was poured into an ice-water solution. Then the resultant solid was filtered off, dried, and crystallized from ethanol to afford **16**. Yield 74%. M p 212 – 214°C. IR (KBr, cm^{-1}) : 3098 (CH - aromatic), 2933, 2894 (CH - aliphatic), 2217 (C≡N), 1775, 1709, 1670 (3C=O), 1587 (C=N). ^{1}H NMR (DMSO-d_6, 500 MHz, δ, ppm): 1.03 (t, 3H, CH_3), 2.07 (m, 4H, $2CH_2$), 4.36 – 4.82 (q, 2H, CH_2), 5.55 (s, 1H, CH), 7.43 –8.00 (m, 8H, aromatic protons). ^{13}C NMR (DMSO-d_6, 125 MHz, δ, ppm): 167.04, 163.90, 159.10, 150.05, 134.70, 134.54, 133.05, 131.54, 128.83, 128.34, 128.05, 127.40, 126.51, 125.52, 123.41(CO and aromatic carbons), 90.09, 50.59, 28.56, 14.46 (aliphatic carbon). Ms, m/z = 414 ($M^{\bullet+}$, 29.68%), *Anal*. Calcd. for $C_{23}H_{18}N_4O_4$ (414.42): C, 66.66%; H, 4.38%; N, 13.52%; O, 15.44%. Found: C, 66.70%; H, 4.35%; N, 13.50%; O, 15.49%.

1-(4-(4-(3-Amino-5-oxo-4,5-dihydro-1H-pyrazol-4-yl)phthalazin-1-yl)phenyl)pyrrolidine-2,5-dione (17)

A mixture of compound **16** (10 mmol) and hydrazine hydrate (10 mmol) in ethanol (20 mL) was heated under reflux for 6 hours. After the obtained solid was collected by filtration, dried, and crystallized from ethanol to give **17.** Yield 71%. M p 258 – 260°C. IR (KBr, cm^{-1}): 3470, 3153 (NH_2), 3100 (NH), 1776 - 1675 (C=O), 1593 (C=N). ^{1}H NMR (DMSO-d_6, 125 MHz, δ, ppm): 2.06 (m, 4H, $2CH_2$), 4.02 (s, 2H, NH_2, exch..), 5.01 (s, 1H, CH), 7.86 – 8.28 (m, 8H, aromatic protons), 11.58 (s, 1H, NH, exch.). Ms, m/z = 400 (M^+, 13.33%), 401 (M + 1, 9.32%), *Anal*. Calcd. for $C_{21}H_{16}N_6O_3$ (400.40): C,63.00%; H, 4.03%; N, 20.99%; O, 11.99%. Found: C, 64.05%; H, 4.15%; N, 20.80%; O, 12.05%.

5-Amino-4-(4-(4-hydrazinylphenyl)phthalazin-1-yl)-2,4-dihydro-3H-pyrazol-3-one (18)

A mixture of chlorophthalazine **3** (10 mmol) and hydrazine hydrate (10 mmol) in *n-butanol* was heated under reflux for 6 hours. After cooling, the reaction mixture was filtered off, dried, and crystallized from ethanol. Yield 85%. M p 253 – 255°C. IR (KBr, cm^{-1}): 3467 - 3312 (NH_2), 3163 (NH) 1738-1701 (C=O), 1596 (C=N). ^{1}H NMR (DMSO-d_6, 400 MHz, δ, ppm): 2.03 (m, 4H, $2CH_2$), 3.40 (s, 2H, NH_2, exch..), 6.99 – 7.55 (m, 8H, aromatic protons), 9.90 (s, 1H, NH, exch..). ^{13}C NMR (DMSO-d_6, 100 MHz, δ, ppm): 167.48, 159.50, 137.59, 135.03, 133.02, 128.83, 127.00, 126.01, 125.60, 123.91, 123.89, 29.26. Ms, *m/z* = 333 ($M^{\bullet+}$, 26.91%), *Anal*. Calcd. for $C_{18}H_{15}N_5O_2$ (333.35): C, 64.86%; H, 4.54%; N, 21.01%; O, 9.60%. Found: C, 64.80%; H, 4.60%; N, 20.90%; O, 9.70%.

2.3 Biological assessment

Antimicrobial assay

Test Method[40]

The antibacterial and antifungal properties of the synthesized compounds were assessed through *in vitro* experiments using nutrient agar and Sabouraud dextrose agar, respectively [40]. The antibacterial evaluation targeted *Staphylococcus aureus* (ATCC:13565) (Gram-positive) and *Escherichia coli* (ATCC:10536) (Gram-negative), while the antifungal activity was tested against *Candida albicans* (ATCC:10231) and *Aspergillus niger (*ATCC:16404*)*. The test solutions were prepared at a concentration of 15 mg/mL, with dimethyl sulfoxide (DMSO) serving as the negative control. For microbial culture preparation, sterilized agar media (20–25 mL per plate) were dispensed into sterile Petri dishes and left to solidify at 25°C. A microbial suspension was prepared in sterile saline and adjusted to match the McFarland 0.5 standard, equivalent to 1.5×10^5 CFU/mL. The turbidity of the suspension was standardized to an optical density (OD) of 0.13 at 625 nm using a spectrophotometer. To ensure uniform microbial distribution, a sterile cotton swab was dipped into the suspension and streaked evenly across the agar surface. After inoculation, the plates were left to dry for 15 minutes. Agar well diffusion was used to evaluate antimicrobial activity, with wells of 6 mm diameter created in the solidified agar using a sterile borer. Each well was filled with 100 µL of the test solution using a micropipette. The plates designated for bacterial testing were incubated at 37°C overnight, while fungal cultures were incubated under appropriate conditions. The experiment was performed in triplicate to ensure reproducibility. The zones of inhibition were measured on a millimeter (mm) scale using a standard ruler throughout this experiment.

2.4 Molecular Docking

Computational methods

Structural data for the selected protein receptors were obtained from the RCSB Protein Data Bank (PDB) as summarized in **Table 1.** Before molecular docking studies, proteins were pre-processed in PyMOL by removing water molecules, ions, and ligands to optimize docking conditions. Synthesized compounds were designed in BIOVIA Draw, and converted to mol2 format via Open Babel [41], and then to pdbqt format using AutoDock Tools for docking readiness. Docking simulations were carried out using AutoDock Vina [42], with compound-specific grid parameters. The resulting protein-ligand interactions were analysed in Discovery Studio, which provided detailed 2D interaction diagrams, revealing key binding affinities and molecular mechanisms behind the compounds' biological activity.

Table 1. Molecular docking targets of antimicrobial activity, PDB IDs, active site coordinates.

Organism		Protein Targets	PDB ID	Active site coordinates:			Reference Ligands
				X	Y	Z	
S. aureus	**G +ve**	Dihydropteroate synthase	**1AD4**	36.04	4.35	36.35	**Ampicillin**
E. coli	**G-ve**	DNA Gyrase	**7P2M**	-17.55	-4.58	12.77	**Gentamicin**
A.niger	**Fungi**	fdc1of A. niger	**4ZA5**	19.95	5.08	20.12	**Nystatin**

3.Results and Discussion

3.1 Chemistry

The synthesis of 1-(4-(4-oxo-3,4-dihydrophthalazin-1-yl) phenyl)-pyrrolidine-2,5-dione (**2**), a key starting material, was efficiently achieved with a good yield through the fusion of succinic anhydride with 4-(4-aminophenyl)phthalazin-1(2H)-one **(1).** The precursor compound **1** was synthesized via the reaction of γ-keto acids with hydrazine hydrate in ethanol, as previously reported [15-16] (*Scheme 1*). The structural elucidation of phthalazine **2** was carried out using various spectroscopic techniques, where the ^{1}H NMR spectrum revealed a characteristic singlet at δ 9.92 ppm, corresponding to the NH proton, while another peak at δ 12.88 ppm was attributed to an OH group. Both signals were exchangeable with D_2O, supporting the presence of tautomeric forms [15,43-46]. The IR spectrum provided further structural confirmation, displaying absorption bands at υ 3467 cm^{-1} and 3158 cm^{-1}, corresponding to the OH and NH, respectively, and a band for C=O at 1780, 1668 cm^{-1}. Reaction of phthalazinone 2 with a mixture of phosphorus oxychloride and phosphorus pentachloride afforded 1-(4-(4-Chlorophthalazin-1-yl)phenyl)pyrrolidine-2,5-dione (3) **[**15**,**43**] (*Scheme 1*).** The latter product was used as a reactive key precursor to synthesize a new series of substituted phthalazine and fused phthalazine derivatives via its reaction with various carbon, nitrogen, oxygen, and sulfur nucleophiles.

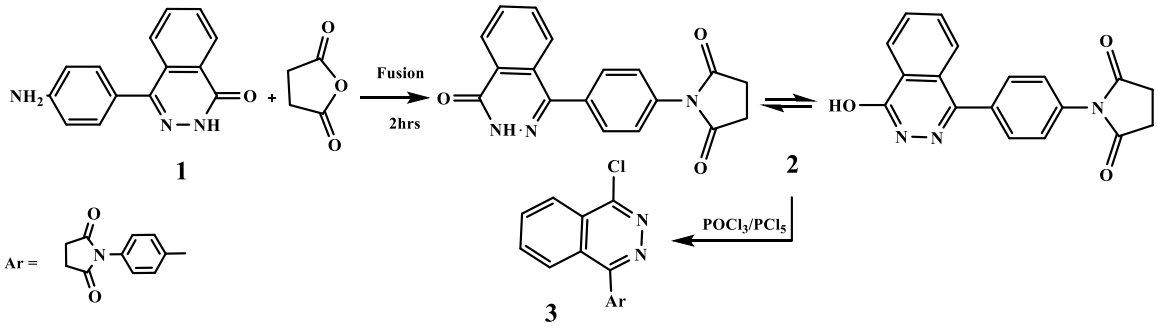

Scheme 1: synthesis of 1-(4-(4-chlorophthalazin-1-yl) phenyl)-1H-pyrrole-2,5-dione (3)

Chlorophthalazine **(3)** served as a key reactive precursor in the synthesis of a novel series of substituted phthalazine and fused phthalazine derivatives. It's remarkable reactivity toward a diverse array of nucleophiles—including carbon, nitrogen, oxygen, and sulfur. Thus, the reaction of chlorophthalazine **(3)** with sodium methoxide [15] in methanol led to the formation of 1-(4-(4-methoxyphthalazin-1-yl) phenyl)pyrrolidine-2,5-dione **(4).** The IR spectrum displayed absorption bands at υ 1383cm^{-1} corresponding to (COC), while ^{1}HNMR showed a signal as a singlet at δ 4.45 *ppm* for (-CH_3). The ^{13}C NMR confirmed the presence of the (CH_3) group at 54.50 *ppm*.

Similarly, when chlorophthalazine **(3)** was treated with sodium azide [43] in dimethyl sulfoxide (DMSO), a cyclization reaction ensued, affording tetrazolophthalazine **(5).** The IR spectrum displayed absorption bands at υ 1591 cm^{-1}corresponding to C=N. The ^{1}H NMR and ^{13}C NMR agreed well with the proposed structure (*cf.* Experimental **5**). The mass spectra showed a molecular ion peak at m/z 433.

On the other hand, treatment of chlorophthalazine **(3)** with ethanolamine [43] in dioxan led to the formation of compound **(6).** The IR spectrum detected absorption bands of (OH) at υ 3445cm^{-1}, 3332 cm^{-1} for (NH), and for (C=O) at υ 1780 to 1626 cm^{-1}, 1588 cm^{-1} due to (C=N). The ^{1}HNMR showed signals at δ ppm 3.66 – 4.40 (m, 4H, 2CH_2-ethyl), 10.89 (s, 1H, NH, exchangeable), 12.90 (s, 1H, OH exchangeable). The ^{13}C NMR displayed signals for aliphatic carbons at δ 28.82, 28.53, 26.68, 26.60 *ppm*. The mass spectra showed a molecular ion peak at m/z 362. To explore further structural modifications, compound **(6)** was subsequently treated with thionyl chloride ($SOCl_2$) [43] in benzene, yielding the corresponding phthalazinium chloride (**7**). This cationic phthalazinium was then treated with potassium carbonate (K_2CO_3) solution, facilitating the deprotonation and formation of the corresponding free base **(8)**. The IR spectrum of derivative (**8**) showed absorption bands at υ 1778 to 1682 cm^{-1} for (C=O), 1592 cm^{-1} due to (C=N). Mass spectra agreed well with the proposed structure (c.f. experimental 8).

Additionally, reaction of chlorophthalazine **(3)** with thiourea [15] in the presence of sodium ethoxide leads to the formation of mercaptophthalazine **(9).** And the structure of phthalazine derivative **9** improved by IR spectrum

showed bands at υ 2553cm^{-1} (SH), 1775 - 1661cm^{-1}, 1592 cm^{-1} (C=N), and 1349cm^{-1} (C=S); also, ^{1}H NMR spectrum showed signal at δ *ppm* 12.88 (s, 1H, SH, exchangeable with D_2O), 7.44 to 8.29 (m, 8H, aromatic protons). The ^{13}C NMR and Mass spectra agreed well with the proposed structure (*cf.* Experimental 9) ***(Scheme 2)***.

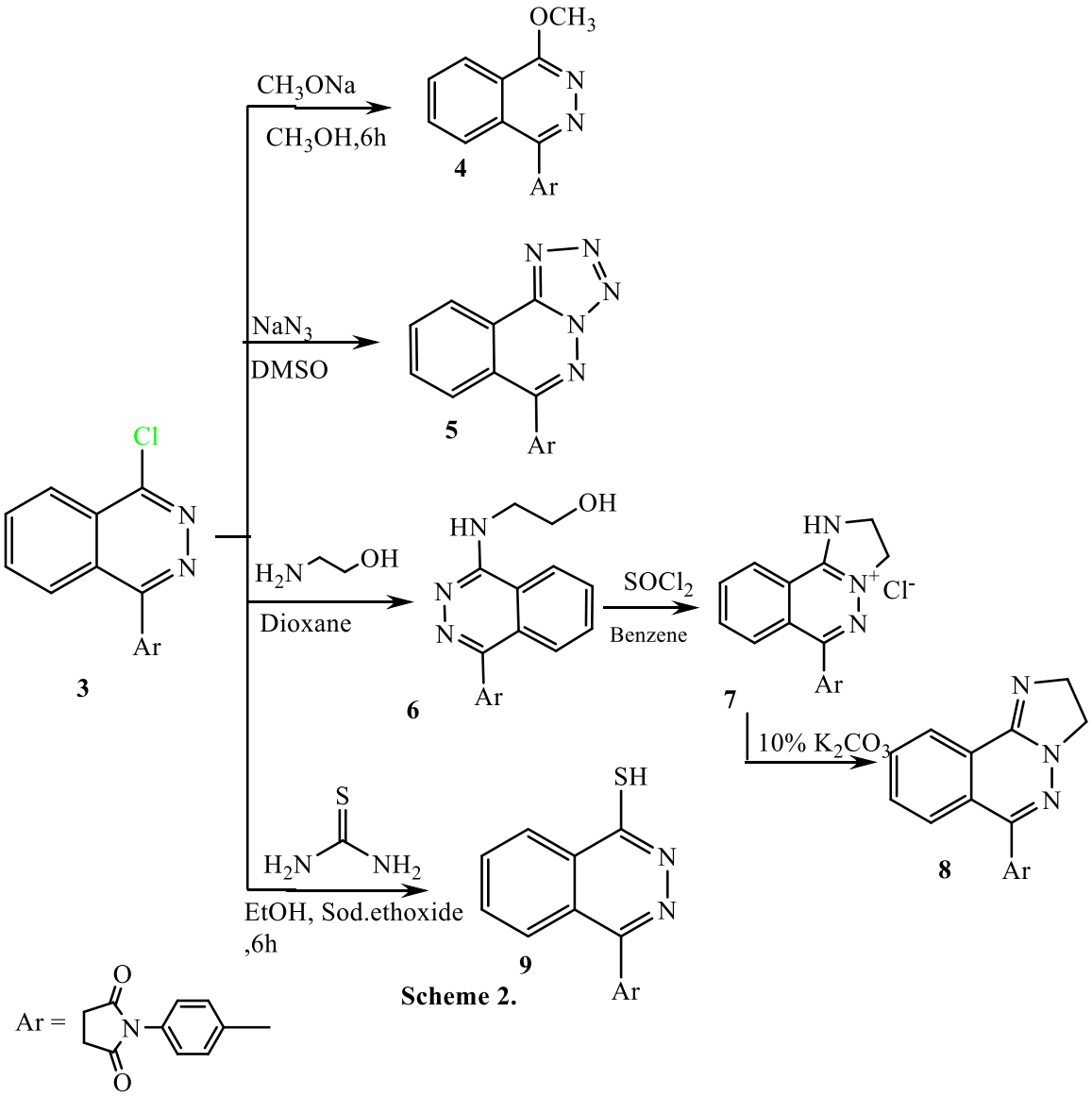

Scheme 2.

The reaction of chlorophthalazine **(3)** with glycine [43] in the presence of pyridine and a trace amount of water afforded the amino acid derivative **(10).** The IR spectrum showed the presence of (OH) at υ 3449 cm^{-1}, and 3166 cm^{-1} for (NH), 1775 to 1665 corresponding to (C=O), 1594 due to (C=N). The ^{1}H NMR detected signals at δ ppm 3.80 (s, 2H, CH_2), 4.43 (s, 1H, NH exchangeable), 6.83 to 7.92 (m, 8H, aromatic protons), 10.88 (s, 1H, OH exchangeable with D_2O). On the other hand, compound **(10)** was subjected to cyclization upon treatment with acetic anhydride [43], yielding the corresponding imidazolidinone derivative **(11).** The IR spectrum of compound **11** confirmed the disappearance of absorption bands of the (OH) and (NH) groups.

In contrast, the fusion of chlorophthalazine **(3)** with anthranilic [43] acid in an oil bath afforded the tetracyclic system (12). The reaction takes place via nucleophilic substitution, followed by a spontaneous ring closure, leading to the formation of an extended conjugated system. The presence of fused ring systems in compound **(12)** was validated through spectral characterization and elemental analysis, confirming the expected structural framework **(***cf* experimental **12).**

While **the** Fusion of chlorophthalazine **3** with ammonium acetate resulted in the formation of amino phthalazine **13**.

Whereas compound **3** underwent reflux with aromatic amines, including *p*-phenylenediamine and *p*-aminophenol, in benzene, resulting in the formation of phthalazine derivatives **14a and 14 b**, respectively. Structures of the products **14a, b** were elucidated based on elemental and spectroscopic analysis (*cf.* Experimental 14a,b). ***(Scheme 3).***

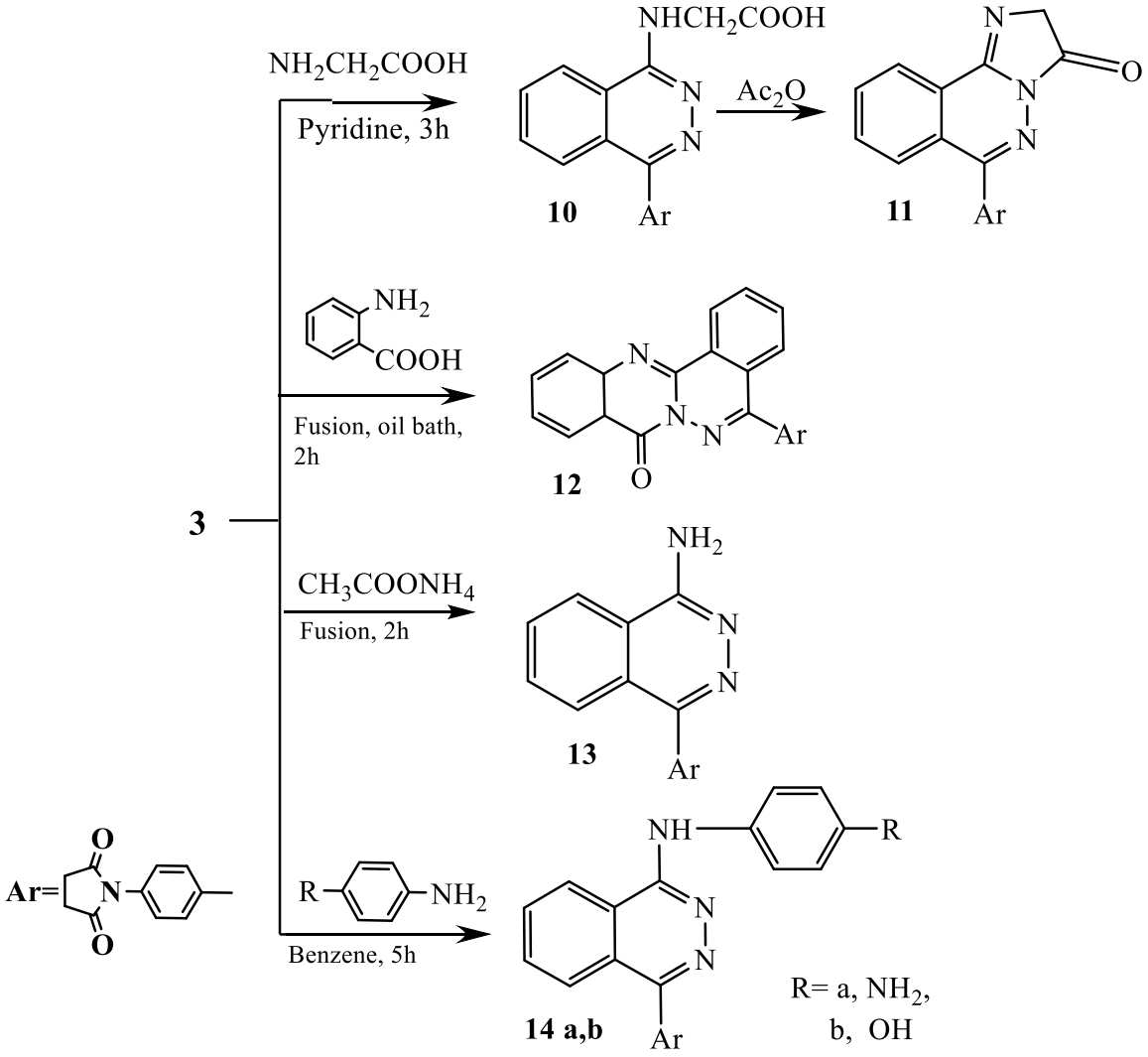

Scheme 3. synthesis of compounds 10-14

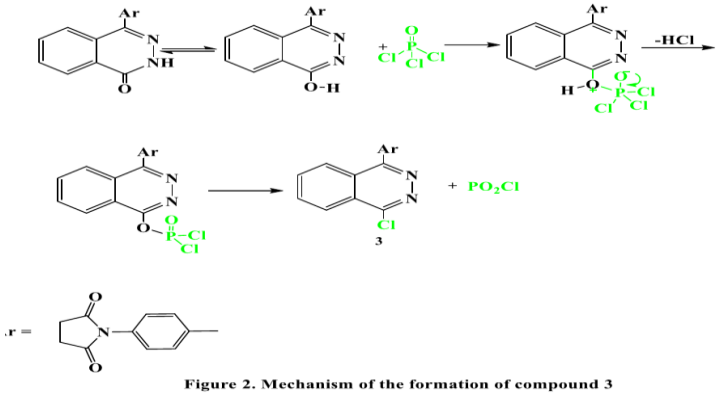

Figure 2. Mechanism of the formation of compound 3

Treatment of cholorophthalazine **3** with thiosemicarbazide [43] under reflux in ethanol due to formation of 1-(4-(3-Amino- [1,2,4] triazolo[3,4-a] phthalazin-6-yl) phenyl)-pyrrolidine-2,5-dione **15**. The IR showed absorption bands of (NH_2) at υ 3464 to 3163cm^{-1}, and for (C=O) at 1775 to 1665 (C=O), 1598 cm^{-1} due to (C=N). When ^{1}H

NMR runs in DSMO displayed signals at δ *ppm* 11.56 (s, 2H, NH_2, exchangeable with D_2O), 7.44 to 8.12 (m, 8H, aromatic protons). Also, ^{13}C NMR showed signals that agreed with the proposed structure (cf. Experimental 15). Mass spectra detected a molecular ion peak at m/z 358.

On the other hand, the reaction of chlorophthalazine **3** with the active methylene compound ethyl cyanoacetate [43], in the presence of sodium ethoxide as a carbon nucleophile, yielded phthalazine derivatives **16.** The IR spectrum displayed the appearance of an absorption band at υ 2217 corresponding to (C≡N), and (3C=O) at 1775, 1709, 1670. The ^1H NMR showed chemical shifts δ *ppm* 1.03 (t, 3H, CH_3), 4.36 – 4.82 (q, 2H, CH_2), 5.55 (s, 1H, CH), 7.43 to 8.00 (m, 8H, aromatic protons). The ^{13}C NMR showed signals that agreed with the proposed structure (cf. Experimental 16). Additionally, the reaction of **16** with hydrazine hydrate [43] in ethanol resulted in the formation of pyrazole derivatives **17**. The IR spectrum showed absorption bands at υ 3470 to 3312 cm^{-1} for (NH_2), 3163 cm^{-1} due to (NH), 1593 cm^{-1} for (C=N), and disappearance of the absorption band of (C≡N). The ^1H NMR displayed signals at δ ppm 4.02 (s, 2H, NH_2, exchangeable with D_2O), 5.01 (s, 1H, CH), 7.86 – 8.28 (m, 8H, aromatic protons), 11.58 (s, 1H, NH, exchangeable).

Furthermore, the reactivity of chlorophthalazine **3** towards primary amines like hydrazine hydrate [43] in *n*-butanol afforded products **18**. Structure of the compound **18** was elucidated based on elemental and spectroscopic analysis (*cf.* Experimental 18) (***Scheme 4***).

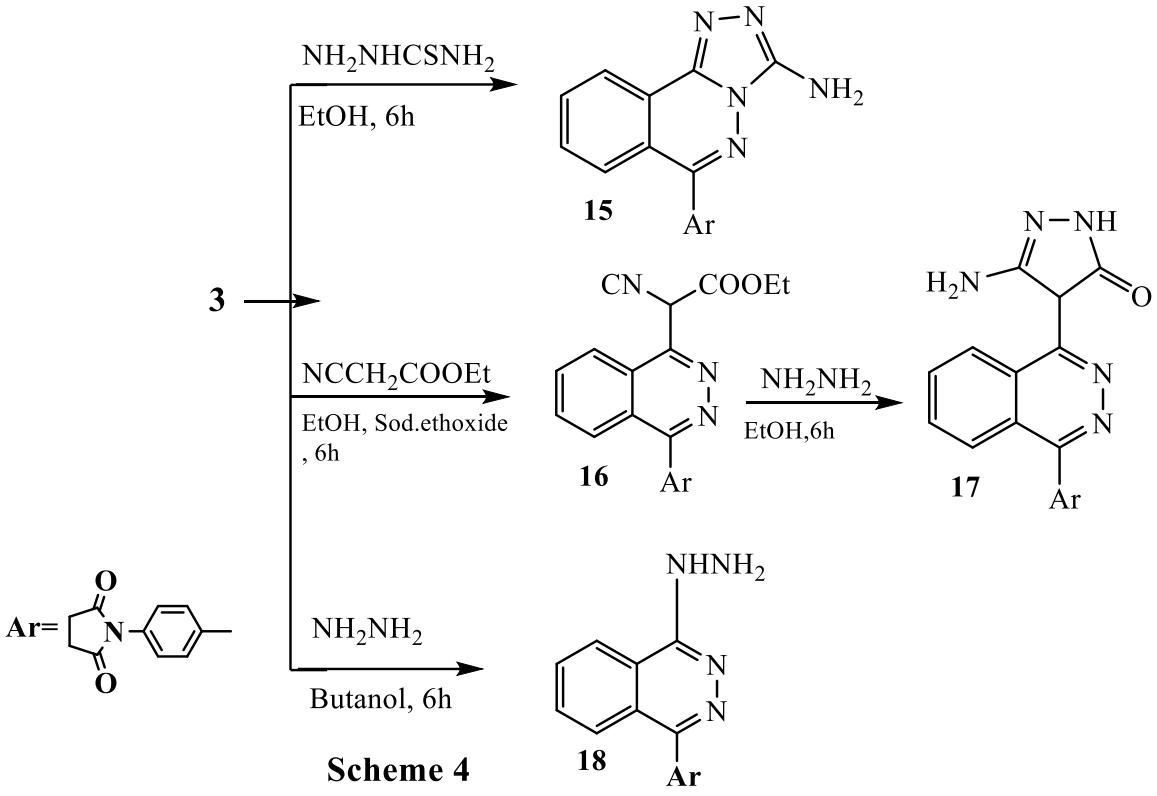

Scheme 4

.

3.2 Antimicrobial assay

In vitro, assessment of antibacterial and antifungal activity of synthesized compounds (1-18) against some of the pathogenic bacteria and fungi

The newly synthesized phthalazine derivatives (**1–18**) were assessed in *vitro* for antibacterial and antifungal activities against selected pathogenic microorganisms. The assessment was carried out using the agar well diffusion method [40]. For antibacterial screening, the compounds were tested against *Staphylococcus aureus* (ATCC 13565), representing Gram-positive bacteria, and *Escherichia coli* (ATCC 10536), representing Gram-negative bacteria. To ensure a comparative analysis, Ampicillin was used as the standard antibiotic for Gram-positive bacteria, while Gentamicin served as the reference for Gram-negative bacterial strains. The antibacterial activity of each compound was determined by measuring the diameter of the inhibition zone (mm), which provides a direct indication of microbial growth suppression. In addition to bacterial screening, the antifungal efficacy of the

synthesized compounds was evaluated against *Candida albicans* (ATCC 10231) and *Aspergillus Niger* (ATCC 16404). The antifungal assay was conducted using Sabouraud dextrose agar (SDA) as the culture medium. Nystatin was employed as the standard antifungal agent to provide a reference for evaluating the potency of the synthesized derivatives. To ensure accuracy and reproducibility, all antimicrobial experiments were performed in triplicate, and the inhibition zone diameters were recorded as mean values with standard deviations (± SD). The summarized results, including inhibition zone diameters for each microorganism, are presented in **Table 2.**

Table 2. The antimicrobial results of the synthesized compounds were measured by the inhibition zone (mm)

Microorganism	Gram-negative bacteria	Gram-positive bacteria	Fungi	
	Escherichia Coli (ATCC:10536)	Staphylococcus Aureus (ATCC:13565)	Candida Albicans (ATCC:10231)	Aspergillus Nigar (ATCC:16404)
Compound No.	**The inhibition zone (mm)**			
1	NA	NA	NA	NA
2	NA	NA	NA	NA
3	**14.3±0.6**	NA	NA	NA
4	**13.3±0.6**	**12±1.0**	NA	NA
5	**17.7±0.6**	NA	NA	NA
6	**14±1.0**	NA	NA	NA
8	NA	NA	NA	NA
9	**11±1.0**	NA	NA	NA
10	**11±1.0**	NA	NA	NA
11	NA	NA	NA	NA
12	NA	NA	NA	NA
13	NA	NA	NA	NA
14a	**12.3±0.6**	**13±1.0**	NA	NA
14b	NA	NA	NA	NA
15	**13±1.0**	**14.3±0.6**	NA	**13±1.0**
16	**11.3±0.6**	NA	NA	NA
17	**18±1.0**	NA	NA	NA
18	**17.3±0.6**	**13±1.0**	NA	NA
Gentamicin	**27±1.0**	-	-	NA
Ampicillin	-	**21.3±0.6**	-	NA
Nystatin			**21.6±0.6**	**19.3±0.6**

NA: no activity. The expression for the zone of inhibition is represented by mean± standard deviation (mm).

Phthalazine derivatives have long been recognized for their diverse pharmacological applications, particularly their antimicrobial potential. The findings, summarized in **Table 2**, the anti-microbial activity results of the examined derivatives, demonstrated that many synthesized compounds showed different inhibition zones versus the selected bacteria and fungi. Among the tested derivatives, compound **15** exhibited remarkable antibacterial potency, displaying broad-spectrum activity against both *Escherichia coli* (inhibition zone 13±1.0 mm) and *Staphylococcus aureus* (inhibition zone 14.3±0.6mm). Interestingly, compound **15** also showed significant antifungal activity against *Aspergillus Niger* (inhibition zone 13±1.0mm), even surpassing the efficacy of Nystatin (inhibition zone 19.3±0.6mm), the standard antifungal agent. Similarly, compounds **4, 14a**, and **18** exhibited notable antibacterial activity, particularly against *Escherichia coli* (inhibition zones 13.3, 12.3, 17.3 ±0.6mm) and *Staphylococcus aureus* (inhibition zones 12, 13, 13±1.0mm). Their effectiveness was found to be comparable or superior to Gentamicin (inhibition zone 27±1.0 mm) and Ampicillin (inhibition zone 21.3±0.6mm). In contrast, compounds **3, 5, 6, 9, 10, 16**, and **17** displayed moderate antibacterial activity against

Escherichia coli with inhibition zones ranging from 11 to 18 mm, but did not exhibit significant antifungal effects. The absence of antifungal activity in these derivatives may be attributed to limited fungal cell penetration or insufficient interaction with fungal enzymatic targets. Conversely, compounds **1, 2, 8, 11, 12, 13**, and **14b** exhibited no detectable antimicrobial activity.

3.3 Molecular Docking Study

3.3.1 Docking and interaction with Dihydropteroate synthase of *S. aureus*:

Dihydropteroate synthase serves as a key enzyme in the folate biosynthesis pathway, a crucial metabolic process necessary for bacterial growth and survival. Consequently, targeting this enzyme presents a viable approach for limiting bacterial proliferation. In this study, molecular docking analyses revealed that compounds **4, 14a, 15**, and **18** exhibited strong binding affinities to dihydropteroate synthase, with binding energies of -6.90, -6.80, -7.90, and -7.20 kcal/mol, respectively. These binding energies surpass that of the reference antibiotic Ampicillin, which demonstrated a lower binding energy of -6.40 kcal/mol (as outlined in **Table 3, Figure 3**). The higher binding affinities of these compounds suggest their potential as effective inhibitors of dihydropteroate synthase. A deeper investigation into the molecular interactions of these compounds revealed their ability to establish hydrogen bonds with key amino acid residues within the enzyme's active site. Specifically, interactions were observed with Arg204, Arg52, Gln105, Lys203, Asp84, Val49, and Asn11, which contribute significantly to ligand stabilization. The presence of these hydrogen bonds strengthens ligand-enzyme binding and enhances inhibitory potential. In addition to hydrogen bonding, the compounds engaged in multiple hydrophobic interactions that further reinforced their binding stability. Alkyl bonding interactions were noted with Lys203, Arg202, and Arg204, while Pi-cation interactions occurred with Arg52 and Arg239. Furthermore, Pi-sulfur interactions were detected with Met128, suggesting a diverse range of molecular interactions that contribute to the overall binding strength of these compounds. Among these interactions, residues such as Arg204, Asp84, and Gln105—located within the catalytic domain of dihydropteroate synthase—played a crucial role in strengthening ligand binding affinity and stability. These key residues are critical for enzyme activity, and their interaction with the tested compounds suggests a strong inhibitory effect that may significantly impair bacterial folate biosynthesis. The findings of this study strongly indicate that these compounds exert their antibacterial effects by targeting and inhibiting dihydropteroate synthase in *Staphylococcus aureus*, thereby disrupting folate biosynthesis and bacterial survival. This proposed inhibitory mechanism aligns with previous research by [38], which utilized molecular docking techniques to analyse small-molecule interactions with *S. aureus* dihydropteroate synthase. The consistency between these findings further supports the potential of these compounds as promising antibacterial agents, warranting further investigation and potential optimization for therapeutic applications.

Table 3: Molecular interactions with the amino acid residues of dihydropteroate synthase from *S. aureus* (PDB ID: 1AD4).

	Protein	Ligand	Hydrophilic Interactions		Hydrophobic Contacts		No. of H-Bonds	No. of Total Bonds	affinity kcal mol-1
			Residue (H- Bond)	Length	Residue (Bond type)	Length			
1	Dihydropteroate synthase of *S. aureus*	4	Arg204 (H- Bond) Arg52 (H- Bond) Gln105 (H- Bond)	2.91 2.61 2.90	Arg52, (Pi-cation) Lys203, (Pi-alkyl) Asn11, (CH-bond)	3.57 5.30 3.72	3	6	-6.90
2		14a	Gln105, (H- Bond) Lys203, (H- Bond)	1.70 2.74	Arg202, (Pi-alkyl) Arg204, (Pi-alkyl)	5.01 5.49	2	4	-6.80
3		15	Arg52 (H- Bond) Asp84 (H- Bond)	2.74 2.14	Arg52, (Pi-Cation) Arg239, (Pi- cation) Arg239, (Pi- cation) Met128, (Pi- sulfur)	4.66 4.85 4.90 2.99	6	10	-7.90
4		18	Val49 (H- Bond) Asn11 (H- Bond) Asp84 (H- Bond) Arg52 (H- Bond) Arg204 (H- Bond)	2.56 2.81 2.96 2.60 3.00	Lys203, (Pi-alkyl) Arg239, (Pi-cation) Arg52, (Pi- cation)	5.38 3.63 3.95	5	8	-7.20
5		Ampicillin	Arg239 (H- Bond) Asn11 (H- Bond) Arg52 (H- Bond) His241 (H- Bond	2.12 2.01 2.90 2.20	Pro216, (Pi-alkyl) Arg202, (Pi-alkyl) His55, (Pi-alkyl) Phe172, (Pi-alkyl) Asn11, (Pi-Pi-T-shaped)	4.30 5.35 4.60 5.40 5.02	4	9	-6.40

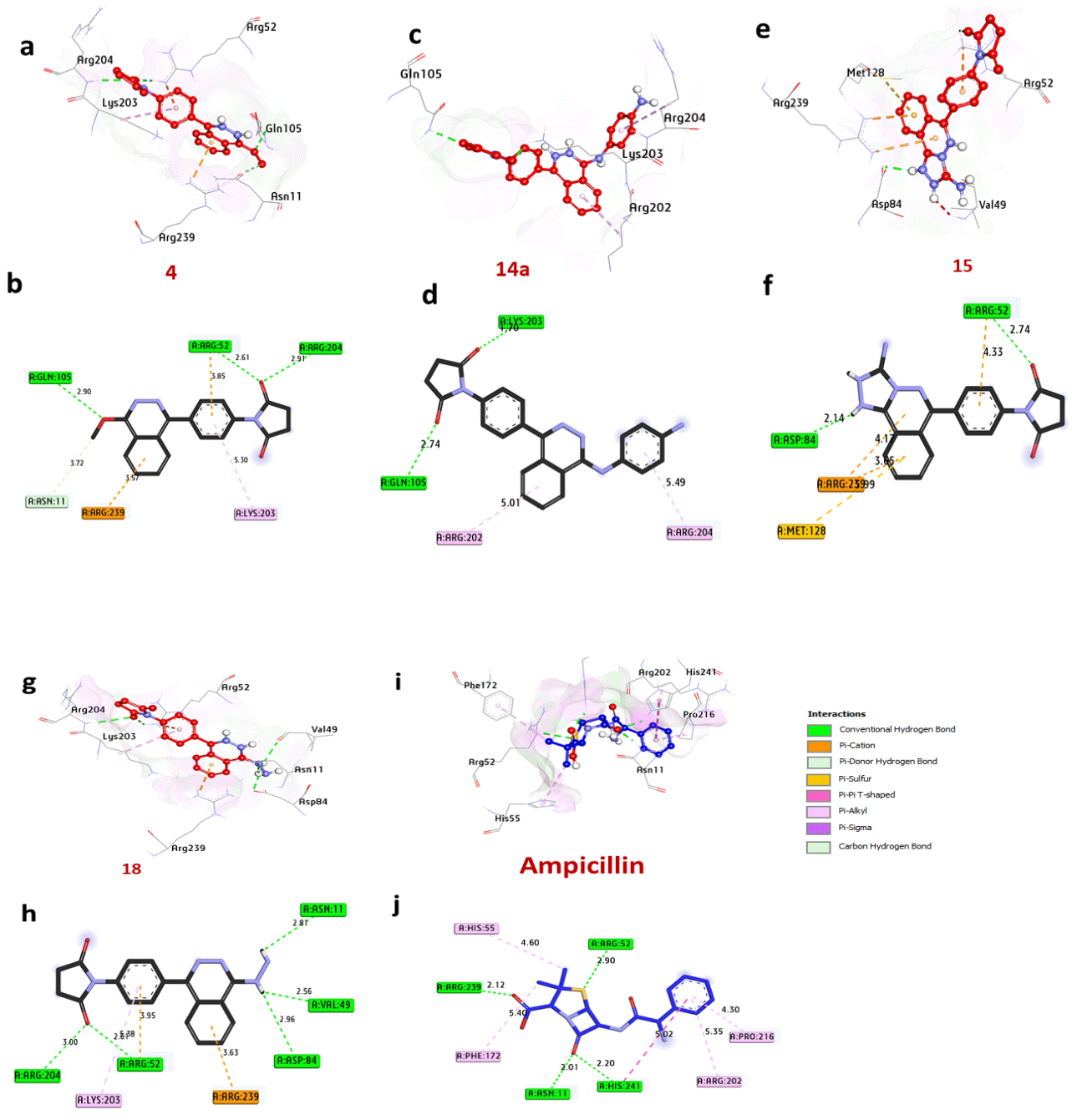

Figure 3. 3D representations of compounds conformations at the binding pocket of dihydropteroate synthase of *S. aureus* (PDB: ID 1AD4): (a and b) **4**, (c and d) **14a**, (e and f) **15**, (g and h) **18,** and (I and j) **Ampicillin**.

3.3.2 Docking and interaction studies with DNA Gyrase of *E. coli*:

To further elucidate the antibacterial potential of the synthesized phthalazine derivatives, molecular docking studies were conducted to assess their interactions with bacterial enzyme targets. As detailed in Table 4 and Figure 4, compounds **4, 14a, 15**, and **18** emerged as highly potent bacterial inhibitors, exhibiting superior binding affinities of -7.50, -7.80, -7.30, and -7.40 kcal/mol, respectively. Notably, these values surpass the binding affinity of Gentamicin (-6.10 kcal/mol), a clinically established antibiotic, highlighting their potential as more effective antibacterial agents. A comprehensive interaction analysis revealed that these compounds establish strong hydrogen bonds with key catalytic residues within the active site of the bacterial enzyme, contributing

significantly to their inhibitory potential. Specifically, crucial interactions were detected with Asp73, Asn46, Arg76, Gly117, Asp49, Thr165, and Val71, residues known to stabilize the ligand-enzyme complex. These interactions likely play a pivotal role in enhancing the binding strength and specificity of these compounds, thereby increasing their potential to disrupt bacterial enzymatic function. Beyond hydrogen bonding, additional stabilizing interactions were observed, further reinforcing the robust binding of these compounds. Arg76, Thr169, and Asp49 engaged in electrostatic interactions, facilitating strong ligand anchoring within the enzyme's active pocket. Moreover, hydrophobic interactions were also detected, including alkyl bonding with Ala47, Val120, Ile78, Ile94, and Pro79, which contribute to ligand stability. Additionally, C-H bonding with Val43, pi-sigma contacts with Ile78 and Ile94, and pi-cation interactions with Glu50 further enhanced ligand binding, collectively strengthening the overall inhibitory effect. One of the most critical observations of this study was the central role of catalytic site residues in promoting ligand binding. Asp73, Asn46, and Glu50 were identified as essential for ligand stabilization, reinforcing their significance in enzyme inhibition and bacterial growth suppression. These residues are conserved across bacterial species, making them promising targets for the rational design of novel antibiotics. The findings of this molecular docking study align with previous research, including a study by [37], which employed computational docking to investigate inhibitor interactions with DNA gyrase and FabH enzymes, both critical targets in bacterial survival. The consistency of these results with prior studies highlights the predictive power of molecular docking in elucidating structure-activity relationships (SARs) and guiding drug design strategies. The strong binding affinities of compounds **4, 14a, 15**, and **18**, along with their ability to interact with key catalytic residues, underscore their potential as lead antibacterial agents. Their capacity to disrupt bacterial enzymatic function, particularly DNA gyrase, suggests that these compounds could serve as promising candidates for further optimization and development in combating bacterial resistance. Future studies focusing on molecular dynamics simulations, ADMET (Absorption, Distribution, Metabolism, Excretion, and Toxicity) profiling, and in vivo efficacy evaluations will be essential to further validate their therapeutic potential.

Table 4: Ligands molecular interactions with amino acids of DNA Gyrase from *E. coli* (PDB ID: 7P2M).

NO	Protein	Ligand	Hydrophilic Interactions		Hydrophobic Contacts		No. of H-Bonds	No. of Total Bonds	affinity kcal mol-1
			Residue (H-Bond)	Length	Residue (Bond type)	Length			
1	DNA Gyrase of *E.coli* (PDB: ID 7P2M)	4	Asp73, (H- Bond) Asn46, (H- Bond) Arg76, (H- Bond)	1.90 2.69 3.36	Ala47, (alkyl) Val120, (alkyl) Ile78, (alkyl) Ile78, (pi-sigma) Met95, (pi-sulfur) Val43, (C-H bond) Glu50,(pi-Cation)	5.48 4.60 5.44 3.51 5.47 3.43 3.82	3	10	-7.50
2		14a	Gly117, (H- Bond) Asn46, (H- Bond)	2.69 2.14	Ile78, (alkyl) Ile94, (alkyl) Ile94, (pi-sigma) Ile94, (pi-sigma)	5.17 5.43 3.90 3.71	2	6	-7.80
3		15	Asp73, (H- Bond) Asp73, (H- Bond)	2.10 2.52	Ile94, (alkyl) Ile78, (alkyl) Ile78, (alkyl) Pro79, (pi-alkyl) Glu50, (pi-Cation) Glu50, (pi-Cation)	4.95 4.85 4.50 4.84 4.00 3.93	2	8	-7.30
4		18	Thr165, (H- Bond) Asn46, (H- Bond) Val71, (H- Bond)	2.19 2.75 2.22	Ala47, (alkyl) Val120, (alkyl) Val167, (alkyl) Ile78, (Pi-sigma) Met95, (pi-sulfur) Asp73, (pi-Cation) Glu50, (pi-Cation)	4.92 4.31 5.37 3.54 5.04 3.91 3.66	4	12	-7.40
5		Gentamicin	Asp49, (H- Bond) Asn46, (H- Bond)	2.19 2.34	Ile94, (alkyl) Ile94, (alkyl) Ile78, (alkyl)	4.24 5.08 5.05	2	6	-6.10

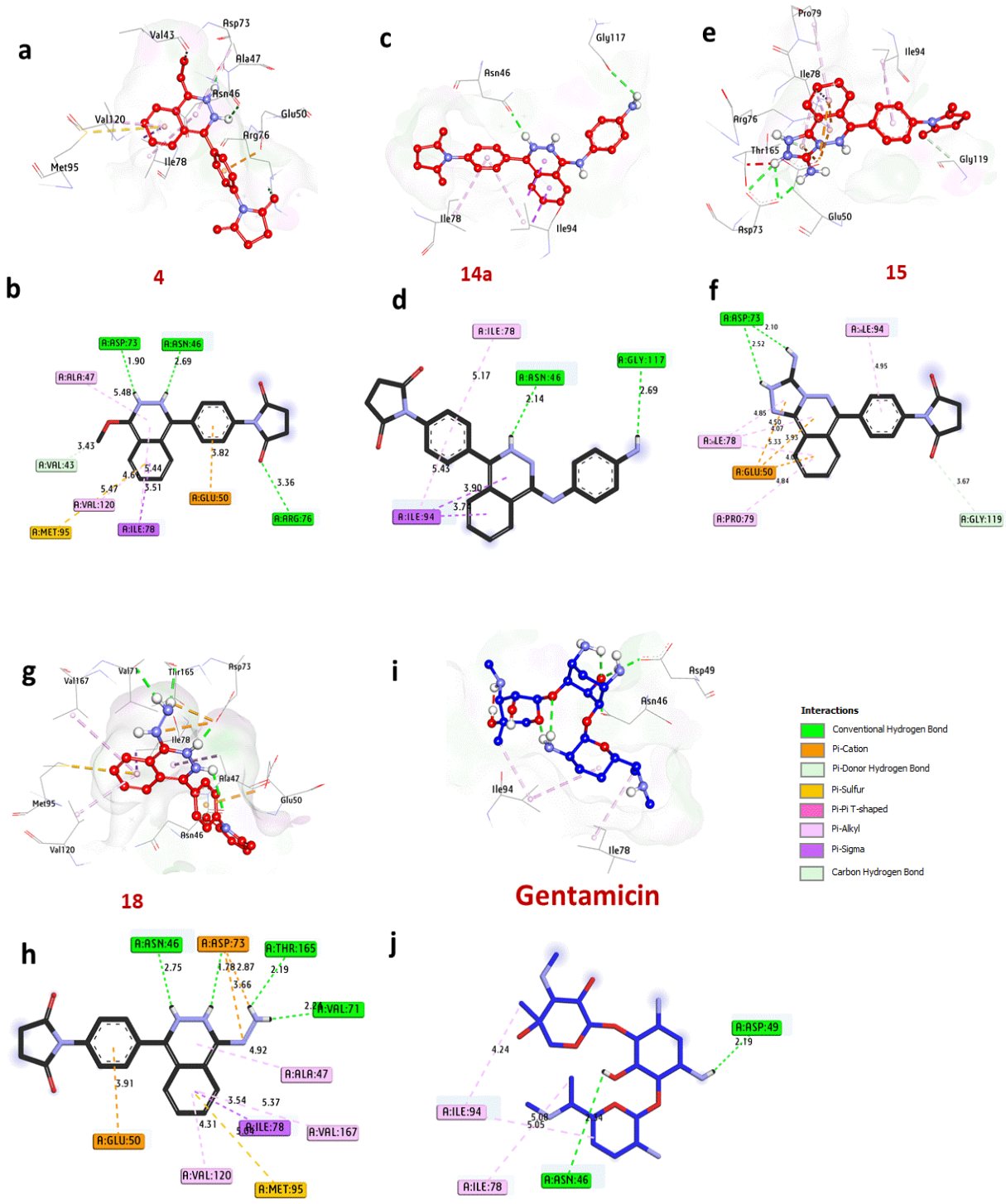

Figure 4: 3D visualizations of compounds within the binding pocket of DNA Gyrase from *E. coli* (PDB ID: 7P2M), displaying (a, b) Compound **4**, (c, d) Compound **14a,** (e, f) Compound **15,** (g, h) Compound **18**, and (i, j) **Gentamicin**.

3.3.3 Docking and interaction with the fdc1 of A. Niger (PDB:ID 43A5):

The development of distinct aromas in fermented beverages, such as wine and beer, is significantly influenced by the enzymatic activity of ferulic acid decarboxylase (FDC1) in *Aspergillus Niger* and the sensory profile of fermented products. Inhibition of FDC1 has been explored as a potential strategy for modulating aroma profiles and controlling fungal growth in industrial fermentation processes. Molecular docking analyses, as illustrated in

Figure 5 and Table 5, revealed that compound 16 exhibited a remarkably high binding affinity of -11.30 kcal/mol, surpassing the binding energy of Nystatin (-10.80 kcal/mol), a well-established antifungal agent. This superior binding affinity suggests that compound **15** may act as an effective inhibitor of fungal FDC1, potentially disrupting its catalytic function. A detailed interaction analysis demonstrated that the strong binding affinity of compound **15** was primarily facilitated by hydrogen bonding with the catalytic residue Ser224, which contributed to enhanced ligand stability within the enzyme's active site. Additionally, multiple hydrophobic interactions were observed, further reinforcing the ligand's strong binding and inhibitory potential. These included alkyl bonding with Cys316, Ile327, and Ile171, pi-cation interactions with Ser224, pi-sigma bonding with Ile171 and Ile327, pi-sulfur interaction with Met326, and carbon-hydrogen bonding with Ser224. These interactions collectively played a significant role in stabilizing compound **15** within the enzyme's active pocket. Notably, key catalytic residues, including Ser224, Val231, and Ile171, were found to be essential for stabilizing the ligand-enzyme complex. Their involvement in hydrogen bonding and hydrophobic interactions underscores their importance in determining the compound's inhibitory potential. The ability of compound **15** to strongly interact with these residues highlights its potential as an effective antifungal agent targeting FDC1. These findings align with a recent study conducted by [48], which demonstrated the antimicrobial efficacy of compounds targeting *A. niger* FDC1 using molecular docking approaches. The alignment between these studies strengthens the hypothesis that compound **15** could serve as a potent inhibitor of fungal FDC1, presenting valuable prospects for antifungal drug development. Furthermore, the ability of compound **15** to modulate FDC1 activity could have implications in food and beverage fermentation, providing a means to fine-tune aromatic profiles by selectively inhibiting specific fungal enzymatic pathways.

Table 5: Interactions at the molecular level with the amino acids of fdc1 of *A. niger* (PDB:ID 4ZA5)

NO	Protein	Compounds	Hydrophilic Interactions		Hydrophobic Contacts		No. of H-Bonds	No. of Total Bonds	affinity kcal mol^{-1}
			Residue	Length	Residue (Bond type)	Length			
1	fdc1of *A. niger* (PDB:ID 5TZ1)	15	Ser224, (H- Bond)	2.85	Cys316, (Pi-alkyl) Ile327, (Pi-alkyl) Ile171, (Pi-alkyl) Met326, (Pi-sulfur) Ile171, (Pi-sigma) Ile327, (Pi-sigma) Ser224, (Carbon H bond) Ser224, (Pi-cation)	5.22 4.81 4.87 5.51 3.79 4.81 3.55 4.59	1	10	-11.30
2		Nystatin	Val231, (H- Bond) Trp166, (H- Bond) Arg173, (H- Bond)	1.93 2.05 2.59	Ile142, (Pi-alkyl)	4.57	3	4	-10.80

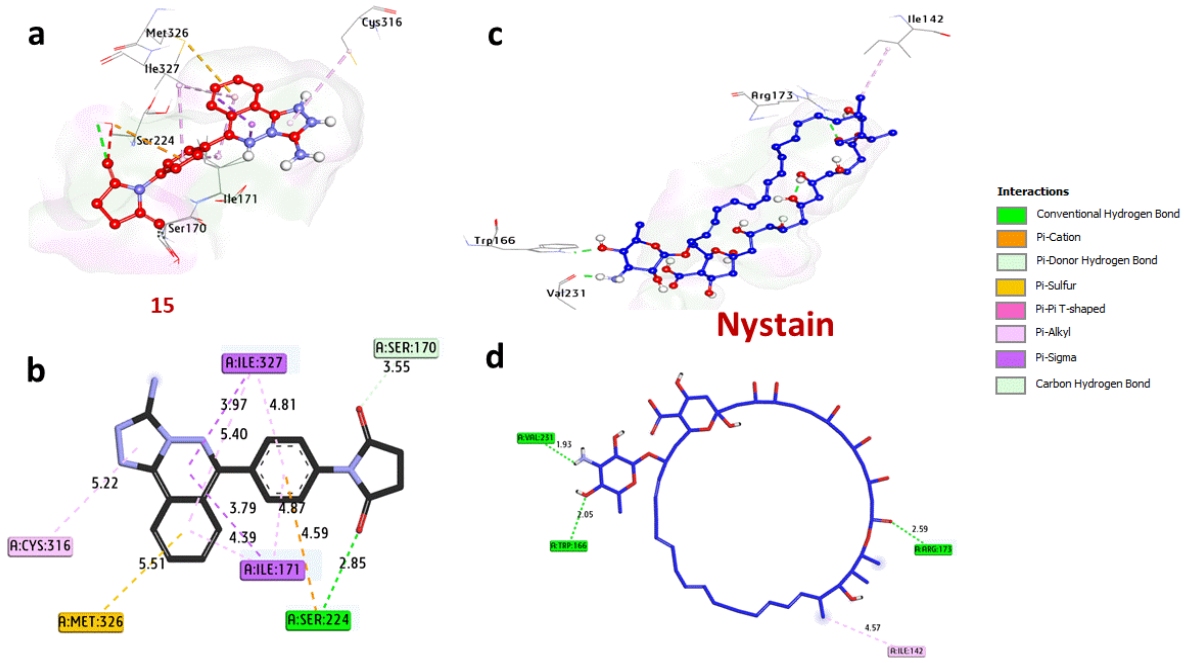

Figure 5: 3D visualizations of compounds within the binding pocket of Fdc1 from *Aspergillus niger* (PDB ID: 4ZA5), showing (a, b) Compound **15** and (c, d) **Nystatin**.

Conclusion

A series of novel phthalazine derivatives incorporating the pyrrolidine-2,5-dione moiety was successfully synthesized with good yields. A variety of elemental and spectral analyses were conducted to verify the structural characterization of these newly developed compounds. Of these, compounds **4, 14a, 15**, and **18** demonstrated dual antimicrobial properties, underscoring their potential as therapeutic agents. The in vitro evaluations of their pronounced efficacy against both bacterial strains (*E. coli*, *S. aureus*) and fungal species (*A. niger*) indicate a broad-spectrum antimicrobial potential. Molecular docking studies further support these findings by demonstrating significant interactions with key microbial enzymes.

Conflicts of Interest

The authors declare that there are no conflicts of interest regarding the publication of this paper.

Acknowledgments

The authors express their gratitude to Benha University, Faculty of Science, and extend their appreciation to the Chemistry Department for their technical support.

References

[1] N. Dhiman, K. Kaur, and V. Jaitak, Bioorg. Med. Chem., 2020, 28(15), 115599.
[2] D. El Sayed, S. M. El Rayes, H. A. Soliman, I. E. AlBalaa, M. S. Alturki, A. H. AlKhzem, M. A. Alsharif, M. S. Nafie, RSC Adv., 2024, 14, 13027.
[3] A. A. H. Abdel-Rahman, S.G. Donia, A. A. F.Wasfy, A. A. Aly, A. Y. El-Gazzar, Der Pharma Chemica, 2013, 5(1),196.
[4] A. A. Aly, A. A. F. Wasfy, Indian Journal of Chemistry - Section B Organic and Medicinal Chem., 2004,43(3),629.
[5] A. A. Hassan, R R. Khattab, A. A. F.Wasfy, K. M. Abuzeid, N. A. Hassan, J. of Hetero. Chem., 2018, 55(4), 907.
[6]. Ł. Balewski, M. Gdaniec, A. Hering , C. Furman, A. Ghinet, J. Kokoszka, A. Ordyszewska, A. Kornicka, Int. J. Mol. Sci. 2024, 25, 11495.
[7] D. Liu, G. Gong, C. Wei, X. Jin, Z.Quan, Bioorg. Med. Chem. Lett., 2016, 26, (6), 1576.
[8] I. E. El-Shamy, A. M. Abdel-Mohsen, A. A. Alsheikh, M. M. G. Fouda, S. S. Al-Deyab, M. A. El-Hashash, J. Jancar, Dyes and Pigments, 2015,113, 357.
[9] I. M. Ghanim, A. A. El Gokha, H. A. A. Abdelaleem, I. E.T. El Sayed, Egypt. J. Chem., 2023, 66(10), 69.
[10] B. Holló, J. Magyari, V. Ž. Radovanović, G. Vučković, Z. D. Tomić, I.M. Szilágyi, G. Pokol, K.M. Szécsény, Polyhedron., 2014, 80, 142.
[11] Y. I. M. Ghanim, A. A. El Gokha , A. H. Abdel Aleem, Egypt. J. Chem. 2025, 68(1), 165.
[12] M. R. Manal, S. Elkhabiry, S. S. Hussein, A. Q. Ghada, Q. Al Anood, Egypt. J. Chem., 2022, 65(13), 331.
[13] B. Đ. Glišić, L. Senerovic, P. Comba, H. Wadepohl, A. Veselinovic, D. R. Milivojevic, M.I. Djuran, J. N. Runic, J. Inorg. Biochem., 2016,155, 115.

[14] M. A. El-hashash, A.Y. Soliman, I. E. EL-Sham, Turk. J. Chem., 2012, 36, 347.
[15] A. F. Wasfy, M. S. Behalo, A. A. Aly, N. M. Sobhi, Chem. Proc. Eng. Res., 2013, 10, 20.
[16] A. F. Wasfy, M. S. Behalo, A. A. Aly, N. M. Sobhi, Der Pharma Chemica, 2013, 5, 82.
[17] K. M. Amin, F. F. Barsoum, F. M. Awadallah, N. E. Mohamed, Eur. J. Med. Chem., 2016, 123, 191.
[18] W. M. Eldehna, S. M. Abou-Seri, A. M. El Kerdawy, R. R. Ayyad, A. M. Hamdy, H. A. Ghabbour, M. M. Ali, D. A. Abou El Ella, Eur. J. Med. Chem., 2016, 50.
[19] J. Xiang, J. Z. Hong, S. Q. Zhe, Med Chem Res., 2017, 26, 193546.
[20] A. A. El-Helby, R. R. Ayyad, H. M. Sakr, A. S. Abdelrahim, K. El-Adl, F. S. Sherbiny, I. H. Eissa, M. M. Khalifa, J. Mol. Str., 2017, 1130, 333.
[21] I. Graça, E. J. Sousa, P. C. Pinheiro and F. Q. Vieira, Oncotarget, 2014, 5(15), 5950.
[22] Z. Malinowski, E. Fornal, A. Sumara, R. Kontek, K. Bukowski, B. Pasternak, D. Sroczynski, J. Kusz, M. Ma ´ łecka and M. Nowak, Beilstein J. Org. Chem., 2021, 17, 558.
[23] S. Tanaka, M. Tanaka, A. Akashi, Stroke, 1989, 20(12), 1724.
[24] S. M. Emam, S. M. E., I. A. I. Ali, H. A. Soliman, M. S. Nafie, BMC Chem., 2023,17(1), 90.
[25] S. M. El Rayes, G. El Enany, I. A. I. Ali, W. Ibrahim, M. S. Nafie, ACS Omega, 2022, 7(30), 26800.
[26] S. Elmeligie, A. M. Aboul-Magd, D. S. Lasheen, T. M. Ibrahim, T. M. Abdelghany, S. M. Khojah, K. A. M. Abouzid, J. Enzyme Inhib. Med. Chem., 2019, 34(1), 1347.
[27] R. Bolteau, F. Descamps, M. Ettaoussi, D.H. Caignard, P. Delagrange, ,P. Melnyk, S. Yous. Eur. J. Med. Chem. 2020, 189, 112078.
[28 M. Wang, C. Liu, L. Dong, X. Jian, Chin. Chem. Lett., 2007, 18 (5),595.
[29] A. A. Wasfy, Heteroatom Chemistry, Volume 14, Issue 7, 2003, 581.
[30] E. F. Ewies, N. F. El-Sayed, M. El-Hussieny, M. S. Abdel-Aziz, Egypt. J. Chem., 2021, 64 (12), 7165.
[31] S. K. Kundu, A. Pramanik, A. Patra, Synlett, 2002, 5, 0823.
[32] H. N. Nguyen, V. J. Cee, H. L. Deak, B. Du, K.P. Faber, H. Gunaydin, B. L. Hodous, S. L. Hollis, P. H. Krolikowski, P. R. Olivieri, The Journal of Organic Chemistry, 2012, 77(8), 3887.
[33] T.G. Chun, K.S. Kim, S. Lee, T.S. Jeong, H.Y. Lee, Y.H. Kim, W.S. Lee, Synthetic Communications, 2004, 34 (7),1301.
[34] M. Yamaguchi, K. Kamei, T. Koga, M. Akima, T. Kuroki, N. Ohi, Journal of medicinal Chem,1993, 36 (25), 4052.
[35] S. Pathak, K. Debnath, S.T. Hossain, S. K. Mukherjee, A. Pramanik, Tetrahedron Letters, 2013, 54(24), 3137.
[36] K. Raval, T. Ganatra, IP International Journal of Comprehensive and Advanced Pharmacology, 2022, 7(1), 12.
[37] F. M. Sroor, A. F. El-Sayed, M. Abdelraof, Archiv Der Pharmazie 2024, 357(6), 2300738.
[38] R. E.Khidre, E. Sabry, A. F. El-Sayed, A. A. Sediek, J. of the Iranian Chemical Society, 2023, 20(12), 2923.
[39] A. H. Jawhari, Y. E. Mukhrish, A. F. El-Sayed, R. E. Khidre, Current Organic Chem., 2023, 27(10), 860.
[40] A. C. Scott, Laboratory control of antimicrobial therapy, Mackie and McCartney: practical medical microbiology, eds Collee J.G., Duguid J.P., Fraser A.G., and Marmion B.P., 13th edn. Churchill Livingstone, Edinburgh, Scotland, 1989,2, 161.
[41] N. M. O'Boyle, M. Banck; C. A. James, C. Morley; T. Vandermeersch; G. R. Hutchison. J. Cheminform. 2011, 3, 33.
[42] J. Eberhardt; D. Santos-Martins; A. F. Tillack; S. Forli; J. Chem. Inf. Model., 2021, 61, 8, 3891.
[43] M. S. Behalo, I. G. El-karim, R. Rafaat,. J. Heterocycl Chem. 2017, 54:3591.
[44] S. A. Rizk, M. F. Youssef, A. M. Mubarak, Egypt.J.Chem, 2020, Vol. 63(5),1767.
[45] M. A. EL-Hashash, M. A. Kadhim, S. A. Rizk, J. Applicable Chem., 2015, 4 (6), 1716.
[46] M. A. El-Hashash, S. A. Rizk, A. A. El-Badawy, J. Het. Chem., 2018, 55 (9), 2090.
[47] M. A. Hawata, A. H. Abdel-Aleem, A. A. Assar, E. F. Elaqsoud, Eur. J. Pharm., and Medical Research, 2018, 5(8), 467.
[48] B. Abd-Elhalim, G. El-Bana, A. El-Sayed, et al. BMC Biotechnol., 2025, 25, 15.